Conformational Flexibility of *o*-Phosphorylcholine and *o*-Phosphorylethanolamine: A Molecular Dynamics Study of Solvation Effects

Thomas B. Woolf† and Benoît Roux*,‡

Contribution from the Research Group on Membrane Transport (GRTM) and Department of Chemistry, Université de Montréal, C. P. 6128, succ. A, Canada H3C 3J7

Received November 11, 1993. Revised Manuscript Received March 30, 1994®

Abstract: The influence of solvent on the conformational flexibility of *o*-phosphorylcholine, $CH_3PO_4^-CH_2CH_2N(CH_3)_3^+$, and of *o*-phosphorylethanolamine, $CH_3PO_4^-CH_2CH_2NH_3^+$, model compounds for the two most common phospholipid headgroups (PC and PE), was explored using molecular dynamics calculations based on a microscopic model with full atomic details. The potential of mean force about the principal dihedral angle, O–C–C–N, was calculated for the model compounds in vacuum and in bulk water using the umbrella sampling technique. In vacuum, the trans conformation is unstable and strongly disfavored with respect to the gauche conformation due to the loss of intramolecular electrostatic interactions. In bulk water, the influence of solvent results in a stabilization of the trans conformation yielding trans/gauche energy differences of +1.5 and +0.02 kcal/mol for the model compounds of PC and PE, respectively. This result is in qualitative agreement with experimental NMR estimates from an analysis based on *J*-coupling constants due to Akutsu and Kyogoku (*Chem. Phys. Lipids* **1977**, *18*, 285–303) and Hauser (*Biochemistry* **1980**, *19*, 366–373). To further understand the nature of solvation effects, the dihedral potential of mean force is calculated for model systems in which the solvent is represented, first, by a vacuum continuum dielectric constant and, second, by a small number of explicit perimary hydration water molecules solvating the phosphate and nitrogen groups. It found empirically that a vacuum continuum dielectric constant of 80 or the presence of 20 explicit primary waters is sufficient to stabilize the trans conformation and reproduce qualitatively the influence of bulk solvation. This suggests that the solvent-induced increased intramolecular conformational flexibility may be equivalently interpreted in terms of continuum dielectric shielding or solvent structure effects by the primary hydration shell. The conformational flexibility of the molecules is further characterized by estimating the transition rate constants between the stable conformations in bulk solvent.

Introduction

The most common headgroups found in biological lipid membranes are phosphorylcholine (PC) and phosphorylethanolamine (PE).[1] For example, in mammalian liver cells, two-thirds of the lipids of the plasma membrane, mitochondria, microsomes, nuclear membrane, and golgi membrane possess one of these two headgroups.[1] The physical state of phospholipid bilayer membranes, as temperature and hydration level are varied, depends to a great extent on the properties of the polar headgroup; for example for equal alkane chain lengths the melting temperature of PE bilayers is higher than that of PC bilayers.[1] Differences in thermodynamic behavior of PC and PE bilayers are traditionally attributed to the differences in size and hydration properties[2] or to the differences in hydrogen bonding abilities of the choline and ammonium groups.[3] Relatively little is known about the hydration of the polar heads of PC and PE lipids at the molecular level and its influence on the physical properties of the membrane. Much effort has been spent to relate the conformations observed in the available crystal structures to the accessible conformations of fully hydrated PC and PE molecules (for an overview see Hauser et al.[4] or Pascher et al.[5]). However, the available crystal structures of DLPE[6,7] and DMPC,[8] which correspond to very low hydration levels, provide little information on the properties of fully solvated phospholipids. The conformational flexibility and the dynamics of the polar moiety of phospholipids have recently been shown to be very sensitive to solvation; in bilayers, a marked change in the deuterium quadrupolar splitting of the methylene groups in the phosphorylcholine headgroups is detected,[9] and the $T1$ relaxation time of the choline methyl groups changes abruptly[10] when the hydration corresponds to less than 20–22 water molecules per lipid. Results obtained from earlier NMR work indicated that the motionally averaged conformation of the polar headgroup of LPPC in solution is consistent with the crystal structure and is independent of the solvent used and of the state of aggregation, suggesting that it is mainly determined by intramolecular forces. Although hydration structures in the neighborhood of the polar heads have also been examined in molecular dynamics simulations of DLPE bilayers, a separation of intramolecular from intermolecular hydration effects was not attempted.[12,13] Thus, a major problem in the interpretation of the experimental as well as the theoretical results remains the separation of solvation effects on the lipid–lipid intermolecular interactions from intramolecular hydration effects on single headgroups.

This theoretical study is concerned with the importance of

† Research Group on Membrane Transport.
‡ Department of Chemistry.
® Abstract published in *Advance ACS Abstracts*, May 15, 1994.

(1) Gennis, R. B. *Biomembranes: Molecular Structure and Function*; Springer-Verlag: New York, NY, 1989.
(2) Blume, A. *Biochemistry* **1983**, *22*, 5436–5442.
(3) Boggs, J. M. *Biochim. Biophys. Acta* **1987**, *906*, 353–404.
(4) Hauser, H.; Pascher, I.; Sundell, S. *Description of Biological Membrane Components by Computer-aided Conformational Analysis*; CRC Press: Boca Raton, FL, 1990.
(5) Pascher, I.; Lundmark, M.; Nyholm, P. G.; Sundell, S. *Biochim. Biophys. Acta* **1992**, *1113*, 339–373.
(6) Hitchcock, P. B.; Mason, R.; Thomas, K. M.; Shipley, G. G. *Proc. Natl. Acad. Sci. U.S.A.* **1974**, *71*, 3036–3040.
(7) Elder, M.; Hitchcock, P.; Mason, R.; Shipley, G. G. *Proc. R. Soc. London A* **1977**, *354*, 157–170.
(8) Pearson, R. H.; Pascher, I. *Nature* **1979**, *281*, 499–501.
(9) Bechinger, B.; Seelig, J. *Chem. Phys. Lipids* **1991**, *58*, 1–5.
(10) Ulrich, A. S.; Volke, F.; Watts, A. *Chem. Phys. Lipids* **1990**, *55*, 61–66.
(11) Hauser, H.; Guyer, W.; Pascher, I.; Skrabal, P.; Sundell, S. *Biochemistry* **1980**, *19*, 366–373.
(12) Raghavan, K.; Reddy, M. R.; Berkowitz, M. L. *Langmuir* **1992**, *8*, 233–240.
(13) Kamodaran, K. V.; Merz, K. M.; Gaber, B. P. *Biochemistry* **1992**, *31*, 7656–7664.

0002-7863/94/1516-5916$04.50/0

solvent effects on the conformational flexibility of o-phosphorylcholine, $CH_3PO_4^-CH_2CH_2N(CH_3)_3^+$, and o-phosphorylethanolamine, $CH_3PO_4^-CH_2CH_2NH_3^+$, model compounds for the two most common polar PC and PE headgroups. Two-dimensional fully relaxed adiabatic potential energy surfaces were calculated as a function of the two main dihedral angles, P–O–C–C and O–C–C–N, for the PC and PE model compounds in vacuum; the potential of mean force along the principal dihedral angle, O–C–C–N, was calculated with umbrella sampling in vacuum and in bulk water; the transition rate constants between the stable conformers in bulk water were estimated. The computational approach chosen here is similar to that employed in other theoretical studies, e.g. the solvation of dimethylphosphate[14] and maltose,[15] the association of Lennard–Jones atoms,[16] amides,[17] and benzene,[18] and the conformational equilibrium of tertiary amides,[19] n-butane,[20] alanine dipeptide,[21-23] and β-turns.[24]

The calculations reveal the important role of solvent in reducing strong intramolecular electrostatic energies. A special effort was made to gain further insight into the nature of hydration effects by considering simplified model systems in which the influence of solvent was approximated by a vacuum continuum dielectric constant and by including a small number of explicit primary hydration water molecules solvating the P and N groups. The results suggest that the solvent-induced increased intramolecular conformational flexibility may be equivalently interpreted in terms of continuum dielectric shielding or solvent structure effects by the primary hydration shell. The microscopic models, potential functions, and computational methodologies are described in the next section. The main results are first outlined briefly and discussed in the following section in more detail. The paper is concluded with suggestions for further experimental and theoretical investigations.

Methodology

Microscopic Models and Potential Function. The two molecules examined in the present study, o-phosphorylcholine and o-phosphorylethanolamine, hereafter referred to as o-PC and o-PE, are shown schematically in Figure 1. The atom and dihedral labeling is based on the convention of Sundaralingam.[25] The o-PC and o-PE molecules are model compounds for the polar headgroups of the two most common phospholipids, phosphorylcholine and phosphorylethanolamine.[1] Both are terminated with a methyl group where the headgroup would normally join to the glycerol group and onto the alkane chains (carbon C1 in Figure 1). The overall conformation and the P-to-N distance of o-PC and o-PE are largely determined by the most important dihedral angles: α_4, P–O12–C11–C12, and α_5, O12–C11–C12–N. Torsions around the remaining dihedral angles are not energetically restricted by significant energy barriers and do not result in an important modification of the overall shape of the molecules. All atoms are included in the microscopic model, including explicitly all the hydrogens of the methyl and methylene groups. In this representation, one o-PC molecule contains 28 atoms and one o-PE molecule contains 19 atoms. We used the potential function developed recently by MacKerrell et al.[26] as part of the parameter set PARM 22[27] of CHARMM[28] (see also Supplementary Material Available below). For the sake of completeness, the partial charges and Lennard–Jones parameters are given in Table 1 for all atoms of both o-PC and o-PE. Briefly, the nonbonded parameters were developed from *ab initio* calculations and free energy calculations with small model compounds. The nonbonded parameters were first adjusted to reproduce interaction energies and optimized geometries of a single water molecule with PO_4^-, NH_4^+, and $N(CH_3)_4^+$ calculated at the *ab initio* level in a variety of orientations; Mulliken populations were used as an initial guess for the partial charges. The partial charges and Lennard–Jones parameters were then refined further using molecular dynamics simulations to reproduce the solvation free energy of these compounds in bulk water. The potential function has been used successfully for simulating DPPC bilayers.[29,30]

The influence of solvent was investigated by considering different simulation systems. A water sphere of 18-Å radius was used to calculate

PC

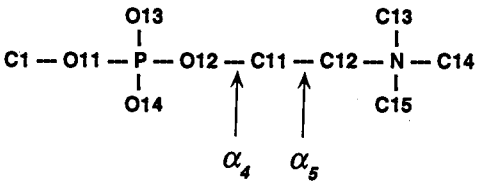

PE

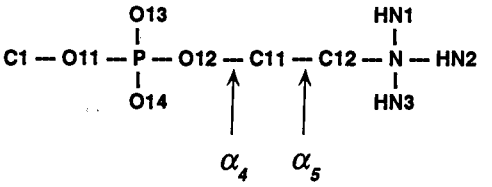

Figure 1. o-Phosphorylcholine (top) and o-phosphorylethanolamine (bottom) molecules, hereafter referred to as o-PC and o-PE, considered in the present study. The atom and dihedral labeling is based on the convention of Sundaralingam.[25] Using this convention, α_4 is the P–O12–C11–C12 dihedral angle and α_5 is the O12–C11–C12–N dihedral angle. The microscopic model used in the simulations includes all hydrogens, but nonpolar hydrogens are not represented in this figure for clarity of presentation.

Table 1. Nonbonded Parameters for o-PC and o-PE

atom	charge (e)	$R_{min}/2$ (Å)	E_{min} (kcal/mol)
Cl	–0.17	2.06	–0.080
H1	0.09	1.32	–0.022
O11	–0.55	1.77	–0.1521
P	1.50	2.15	–0.585
O13	–0.80	1.70	–0.120
O14	–0.80	1.70	–0.120
O12	–0.55	1.77	–0.1521
C11	–0.08	2.175	–0.055
H11	0.09	1.32	–0.022
C12 (PE)	0.13	2.175	–0.055
H12	0.09	1.32	–0.022
N	–0.30	1.85	–0.20
HN1	0.33	0.2245	–0.046
C12 (PC)	–0.10	2.175	–0.055
H12	0.25	0.70	–0.046
N	–0.60	1.85	–0.20
C13	–0.35	2.06	–0.08
H13	0.25	0.70	–0.046

(14) Jayaram, B.; Mezei, M.; Beveridge, D. L. *J. Comput. Chem.* **1987**, *8*, 917–942.
(15) Brady, J. W.; Schmidt, R. K. *J. Phys. Chem.* **1993**, *97*, 958–966.
(16) Straub, J.; Berne, B. *J. Chem. Phys.* **1988**, *89*, 4833–4847.
(17) Jorgensen, W. L. *J. Am. Chem. Soc.* **1989**, *111*, 3770–3771.
(18) Jorgensen, W. L.; Severance, D. L. *J. Am. Chem. Soc.* **1990**, *112*, 4768–4774.
(19) Duffy, E. M.; Severance, D. L.; Jorgensen, W. L. *J. Am. Chem. Soc.* **1992**, *114*, 7535–7542.
(20) Tobias, D. J.; Brooks, C. L., III. *J. Chem. Phys.* **1990**, *92*, 2582–2592.
(21) Mezei, M.; Mehrotra, P. K.; Beveridge, D. L. *J. Am. Chem. Soc.* **1985**, *107*, 2239–2245.
(22) Anderson, A. G.; Hermans, J. *Proteins* **1988**, *3*, 262–265.
(23) Tobias, D. J.; Brooks, C. L. *J. Chem. Phys.* **1990**, *92*, 2582–2592.
(24) Tobias, D. J.; Sneddon, S. F.; Brooks, C. L. *J. Mol. Biol.* **1990**, *216*, 783–796.
(25) Sundaralingam, M. *Ann. N.Y. Acad. Sci.* **1972**, *195*, 324–355.
(26) Schlenkrich, M.; Brickmann, J.; MacKerell, A. D., Jr.; Karplus, M. In Preparation.
(27) Mackerell, A. D., Jr.; Bashford, D.; Bellot, M.; Dunbrack, R. L.; Field, M. J.; Fischer, S.; Gao, J.; Guo, H.; Joseph, S.; Ha, L.; Kuchnir, K.; Kuczera, F. T. K.; Lau, C.; Mattos, S.; Michnick, D. T.; Nguyen, T.; Ngo, B.; Prodhom, B.; Roux, M.; Schlenkrich, J.; Smith, R.; Stote, J.; Straub, J.; Wiorkiewicz-Kuczera, Karplus, M. *Biophys. J.* **1992**, *61*, A143.
(28) Brooks, B. R.; Bruccoleri, R. E.; Olafson, B. D.; States, D. J.; Swaminathan, S.; Karplus, M. *J. Comput. Chem.* **1983**, *4*, 187–217.
(29) Venable, R. M.; Zhang, Y.; Hardy, B. J.; Pastor, R. W. *Science* **1993**, *262*, 223–226.
(30) Heller, H.; Schaefer, M.; Schulten, K. J. *J. Chem. Phys.* **1993**, *97*, 8343–8360.

Table 2. Potential of Mean Force (kcal/mol)

	o-phosphorylcholine				o-phosphorylethanolamine			
system	$\delta W_{t/g}$	$\Delta W^{\ddagger}_{gt}$	$\Delta W^{\ddagger}_{tg}$	$\Delta W^{\ddagger}_{cis}$	$\delta W_{t/g}$	$\Delta W^{\ddagger}_{gt}$	$\Delta W^{\ddagger}_{tg}$	$\Delta W^{\ddagger}_{cis}$
bulk water (MD)	1.5	1.9	0.4	3.8	0.02	2.1	2.1	2.7
bulk water (exp)	2.7[a]				1.3[b]			
vacuum ($\epsilon = 80$)	2.4	2.7	0.3	3.1	0.3	2.1	1.8	2.9
20 primary waters	1.8	2.1	0.3	3.6	1.5	2.8	1.3	2.3

[a] Experimental value from ref 11. [b] Experimental value from ref 43.

the radial distribution functions around the o-PC and o-PE molecules. A smaller water sphere of 13-Å radius was used to calculate the α_5 dihedral potential of mean force and diffusion constant in bulk solution. The TIP3P water model was used.[31] Two types of simplified model systems were considered: in vacuum with a continuum dielectric constant (no explicit waters) and in reduced systems with a small number n of explicit waters surrounding the o-PC and o-PE molecules. Two-dimensional α_4–α_5 adiabatic potential energy surfaces and the potential of mean force were calculated for the isolated molecules in vacuum with dielectric constants of 1, 10, and 80. Finally, the potential of mean force was calculated for the reduced systems with 11 and 20 primary waters (see Table 2).

Potential of Mean Force (PMF). The standard "umbrella samping technique" of Torrie and Valleau[32] was used to determine $W(\alpha_5)$, the PMF along the dihedral angle α_5 of the o-PC and o-PE molecules. Because the present implementation differs slightly from the original formulation,[32] in particular the approach to unbias and match the various windows (see below), it is briefly summarized here for the sake of completeness (in the following, the subscript 5 on α_5 is omitted for clarity). In the present investigation, harmonic window potentials $w_i(\alpha)$ of the form $(1/2)k[\alpha - \alpha(i)]^2$ were used. The unbiased PMF estimate $W_i(\alpha)$, extracted from the ith biased distribution $\langle\rho(\alpha)\rangle_{(i)}$, is

$$W_i(\alpha) = -k_B T \ln[\langle\rho(\alpha))_i] - w_i(\alpha) + C_i \qquad (1)$$

where the constant $C_i = k_B T \ln[\langle\exp[-\beta w_i(\alpha)]\rangle]$. To combine the results from different windows, it is sufficient to determine the relative value of the constants, i.e., $C_i = [C_i - C_{i-1}] + ... + [C_3 - C_2] + [C_2 - C_1] + C_1$, leaving only one arbitrary constant, C_1, to be determined. The relative constant $[C_i - C_j]$ is $-k_B T \ln\langle\exp[-\beta(w_i - w_j)]\rangle_{(j)}$, the free energy difference between the ith and jth window potential. To obtain the final unbiased estimate of the PMF, the estimates from the different windows, $W_i(\alpha)$, were combined by a weighted average proportional to the relative occurrence in the biased distribution function, i.e.,

$$W(\alpha) = \sum_i W_i(\alpha)\left[\frac{\langle\rho(\alpha)\rangle_{(i)}}{\sum_j\langle\rho(\alpha)\rangle_{(j)}}\right] \qquad (2)$$

Equation 2 results in a smooth function $W(\alpha)$ over the whole range of α, giving more weight to the estimate of the ith window, where the enhanced biased distribution, $\langle\rho(\alpha)\rangle_{(i)}$, is statistically more important. This procedure for unbiasing and combining the windows to obtain the PMF differs from the formulation of Torrie and Valleau based on a matching of nearby windows[32] and is similar to the method used by Haydock et al.[33]

Transition Rate Constant. The isomerization rate constants were calculated using the Kramers–Smoluchowsky approximation,[34]

$$k = [\int_{\text{reactant}}^{\text{product}} d\alpha\, D(\alpha)^{-1} e^{+W(\alpha)/k_B T}]^{-1}[\int_{\text{well}} d\alpha\, e^{-W(\alpha)/k_B T}]^{-1}$$
$$\simeq D_b \frac{|W_b'' W_w''|^{1/2}}{2\pi k_B T} e^{-\Delta W^{\ddagger}/k_B T} \qquad (3)$$

where $\Delta W^{\ddagger}$ is the free energy of activation, D_b is the diffusion constant at the transition state, and W_b'' and W_w'' are the second derivative of the potential at the barrier top and in the bottom of the well, respectively. The diffusion constant at the barrier top, D_b, is extracted from the Laplace transform of the memory function, $M(t)$, through Einsten's relation in the limit of $s \to 0$, i.e., $D_b = k_B T/\hat{M}(s)$. Using a formulation due to Straub and Berne,[16,35,36] the memory function at the barrier top is calculated from a trajectory generated in the presence of a harmonic restraining window potential, $(1/2)k(\alpha - \alpha_b)^2$, similar to the one used in the PMF calculations (see above). It is assumed that the dynamics of the restrained dihedral angle follows a generalized Langevin equation for a harmonic oscillator in the neighborhood of the transition state,

$$\frac{k_B T}{\langle\dot{\alpha}^2\rangle}\dot{C}(t) = -\frac{k_B T}{\langle\delta\alpha^2\rangle}\int_0^t C(t')\,dt' - \int_0^t M(t-t')\,C(t')\,dt' \qquad (4)$$

where $C(t)$ is the time correlation function of the velocity of the dihedral angle and $\delta\alpha$ is the deviation of the dihedral around its average. Using the Laplace transform to solve eq 4, it is found that

$$\hat{D}(s) = \frac{-\hat{C}(s)\langle\delta\alpha^2\rangle\langle\dot{\alpha}^2\rangle}{\hat{C}(s)[s\langle\delta\alpha^2\rangle + \langle\delta\dot{\alpha}^2\rangle/s] - \langle\delta\alpha^2\rangle\langle\delta\dot{\alpha}^2\rangle} \qquad (5)$$

where all averages are calculated in the presence of the biasing harmonic potential at the transition state. Finally, the classical transition state theory rate constants (TST),[37,38]

$$k = (1/2)\langle|\dot{\alpha}|\rangle e^{-W_t/k_B T}[\int_{\text{well}} d\alpha\, e^{-W(\alpha)/k_B T}]^{-1} \qquad (6)$$

were calculated for comparison.

Computational Details. A bulk solvent system was constructed from an 18-Å-radius sphere containing 725 TIP3P waters[31] equilibrated at 300 K with the stochastic boundary method.[39] Initial configurations were constructed by placing the o-PC and o-PE molecules at the center and removing the overlapping water molecules. Since the volumes of o-PC and o-PE are approximately 218 and 164 Å^3, seven waters were deleted for o-PC and six for o-PE. Langevin dynamics was used, with stochastic frictional forces corresponding to a relaxation time of 5 ps^{-1} applied only to those water oxygens with distances greater than 14 Å from the center of the sphere. The nonbonded interactions were cut off at 11.0 Å with a smooth switching region of 4 Å. A weak harmonic constraint of 1 kcal/(mol·Å^2) was applied to the center of mass of the o-PC/o-PE molecule to prevent large displacements within the boundary region of the simulation system. All bonds involving hydrogen atoms were constrained with SHAKE.[40]

The PMF of o-PC and o-PE in bulk solution, $W_{\text{bulk}}(\alpha_5)$, and the rate constants were calculated in a water sphere with a radius of 13 Å. Allowing for the volume of the o-PC/o-PE molecules, the total number of water molecules was 253 (o-PC) and 254 (o-PE). The system was first minimized for 5000 ABNR steps and then equilibrated for 50 ps. The protocol for generating each production window involved a 25-ps data collection interval, followed by 1 ps of equilibration for the next window. For the umbrella sampling, a harmonic window potential of 0.015 kcal/mol deg^2, centered around successive values of α_5, was used. To have sufficient overlap between the neighboring biased distribution functions of α_5, the successive windows were separated by 10-deg increments. The final unbiased PMF was determined from 36 windows using eq 2; the 360-deg periodicity and the inversion symmetry at 180° were exploited to increase the statistical convergence. The same simulation systems were used to calculate the value of the diffusion constant at the gauche–

(31) Jorgensen, W. L.; Impey, R. W.; Chandrasekhar, J.; Madura, J. D.; Klein, M. L. *J. Chem. Phys.* **1983**, *79*, 926–935.
(32) Torrie, G. M.; Valleau, J. P. *Chem. Phys. Lett.* **1974**, *28*, 578–581.
(33) Haydock, C.; Sharp, J. C.; Prendergast, F. G. *Biophys. J.* **1990**, *57*, 1269–1279.
(34) Kramers, H. A. *Physica* **1940**, *7*, 284–304.
(35) Straub, J. E.; Borkovec, M.; Berne, B. J. *J. Phys. Chem.* **1987**, *91*, 4995–4998.
(36) Berne, B. J.; Borkovec, M.; Straub, J. E. *J. Phys. Chem.* **1988**, *92*, 3711–3725.
(37) Chandler, D. *J. Chem. Phys.* **1978**, *68*, 2959–2970.
(38) Glasstone, S.; Laidler, K. J.; Eyring, H. *Theory of rate processes*; McGraw-Hill: New York, 1941.
(39) Brunger, A.; Brooks, C. L., III, Karplus, M. *Chem. Phys. Lett.* **1984**, *105*, 495–500.
(40) Gunsteren, W. F.; Berendensen, H. J. C. *Mol. Phys.* **1977**, *34*, 1311–1327.

trans and cis transition states. A dihedral harmonic force constant of 0.061 kcal/(mol·deg^2) and the application of stochastic frictional forces corresponding to a relaxation time of 20 ps^{-1} on the water oxygens located at distances greater than 9 Å from the center of the sphere were used.[39] The velocity autocorrelation function was calculated as a direct average, from 500-ps trajectories, for the gauche–trans and the gauche–gauche barriers. The Laplace transform was calculated numerically from the velocity autocorrelation function using a trapezoidal rule; the discrete sum was truncated at a maximum time of 5 ps. Because the Laplace transform of the velocity autocorrelation function and the inverse of the memory function in eq 5 become progressively more inaccurate as s tends to 0, the value of D was obtained by performing a linear fit to $\hat{D}(s)$ for moderate s values and extrapolating to small values of s.

The PMF of o-PC and o-PE was also calculated for two types of simplified model systems, i.e., in vacuum with a continuum dielectric constant ϵ and in reduced systems with a small number n of explicit waters, hereafter referred to as $W_{vac}(\alpha_5; \epsilon)$ and $W_{prim}(\alpha_5; n)$, respectively. The protocol used to calculate the PMF for the model systems was similar to that described above. For each window, the system was first energy minimized and then equilibrated with Langevin dynamics. For the dielectric continuum calculations, the data collection window was 100 ps, and the PMF was generated with dielectric constants of 1, 10, and 80. Reduced model systems, with 20 and 11 primary waters, were constructed for the o-PC and o-PE molecules. On the basis of the radial distribution functions calculated in bulk water, 8 waters were placed on the PO_4^- phosphate group (3 waters each for O13 and O14, 1 water each for the O11 and O12 oxygens), and 3 or 12 waters around the NX_3^+ of the choline or ammonium group. The data collection window was 50 ps. The initial positions for these reduced explicit waters were obtained from the bulk simulation systems. Throughout the trajectories calculated with the reduced systems, the primary water molecules were maintained in the hydration shell of either the N or the P by applying a half-harmonic restraining potential of the form $K(r - r_0)^2$, for $r > r_0$, and 0 otherwise, with K = 5 kcal/(mol·Å^2) and r_0 = 6 Å to the water oxygen solvated group distance.

To calculate the two-dimensional adiabatic potential energy surface at each point α_4 and α_5, the following protocol was adopted. First, an initial geometry was constructed from internal coordinates, then the position of the atoms not involved directly in the α_4 and α_5 dihedrals was optimized (O11, P, O12, C11, and C12 were kept fixed), and finally, the geometry of the whole molecule was optimized in the presence of harmonic energy constraints to maintain the values of α_4 and α_5 near their prescribed values (the contribution of the harmonic restraint is not included in the final energy). The adiabatic surfaces were calculated every 10° for the dihedral angles between 0 and 360° (1296 conformers were optimized for each molecule). The ABNR energy minimization algorithm was used for the geometry optimizations.[28]

Results

o-PC and o-PE in Vacuum. In this section, the results concerning the flexibility of o-PC and o-PE in vacuum with continuum dielectric constants ϵ of 1, 10, and 80 are described. The α_4–α_5 adiabatic potential energy surfaces and the vacuum PMF of o-PC and o-PE, $W_{vac}(\alpha_5; \epsilon)$, are shown in Figures 2 and 3. The geometries and relative energies of the stable conformations are summarized in Table 3. The vacuum model with a dielectric constant ϵ = 1 corresponds to the isolated molecule in the gas phase, e.g., as it would be studied with *ab initio* calculations.[41,42] Although the vacuum models with an artificially increased dielectric constant do not represent a realistic physical situation, they help in revealing the dominant role played by the intramolecular electrostatic interactions. First, the results with ϵ = 1 are discussed, and then the effect of larger ϵ is described.

The adiabatic surfaces of o-PC and o-PE, shown at the top of Figure 2, have multiple minima separated by large energy barriers; o-PC and o-PE have six and four stable conformers, respectively. For o-PE, the energy minimum observed at (α_4 = 276, α_5 = 67) corresponds to the most stable conformer, labeled gauche-1 in Table 3; the gauche-2 conformer has a marginal stability. For o-PC, the gauche-1 and gauche-2 conformers are the most stable,

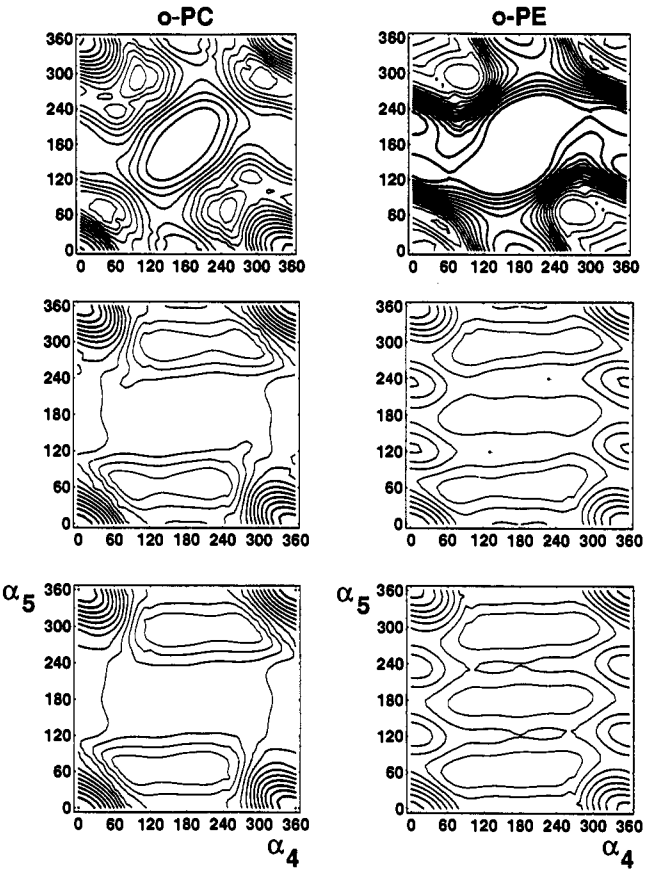

Figure 2. Adiabatic energy surfaces of α_4 and α_5 calculated for o-PC and o-PE in vacuum with continuum dielectric constants of 1, 10, and 80. This figure shows the contour levels at energies from 2 to 30 kcal/mol spaced every 2 kcal/mol with increasingly thick lines. There is a large electrostatic barrier in the all-trans state with a dielectric constant of 1 for both o-PC and o-PE. With dielectric constants of 10 or 80, the size of the trans barrier is significantly reduced, and the α_4 dependence is much broadened. There is symmetry about the diagonal from (0,360) to (360,0). Table 3 summarizes the energetics of the stable conformations observed in this figure.

although the gauche-3 conformer found near (α_4 = 291, α_5 = 124) also appears in $W_{vac}(\alpha_5; \epsilon = 1)$ (see below). The various gauche conformers of o-PC are stabilized by intramolecular hydrogen bonds involving the O13 or O14 oxygens and the hydrogens of the choline group; this is made possible by the larger size of the N group in o-PC relative to o-PE. For example, the gauche-1 conformer is stabilized by several hydrogen bonds involving the O14, O12, and O11 oxygens and two methyl groups of the choline, while the gauche-2 form is stabilized by hydrogen bonds between the O13 and O12 oxygens and a single methyl group of the choline. The PMF, $W_{vac}(\alpha_5; \epsilon = 1)$, shown in Figure 3, has large trans barriers and smaller cis barriers; the gauche conformers, with α_5 near ±60°, are the most stable, in accord with the α_4–α_5 adiabatic surface. In addition, local minima in the PMF of o-PC are also observed at α_5 near 124 and near 236°, in accord with the existence of the gauche-3 conformer found in the adiabatic energy surface. For o-PE, the marginally stable gauche-2 conformer does not give rise to such a feature in the PMF. For both o-PC and o-PE, the large energy barrier in the trans conformation, for which the P-to-N distance is the largest, is primarily due to the loss of intramolecular electrostatic interactions between the P and N groups; the cis conformation of α_4 and α_5 is unfavorable due to bad steric contacts between the phosphate oxygens and the groups on the nitrogen. Similar conclusions were reached by Pullman et al. using *ab initio* calculations based on closely related model compounds of PC and PE.[41,42] In fact, the adiabatic surfaces calculated with ϵ =

(41) Pullman, B.; Berthod, H. *FEBS Lett.* **1974**, *44*, 266–269.
(42) Pullman, B.; Berthod, H.; Gresh, N. FEBS *Lett.* **1975**, *53*, 199–204.

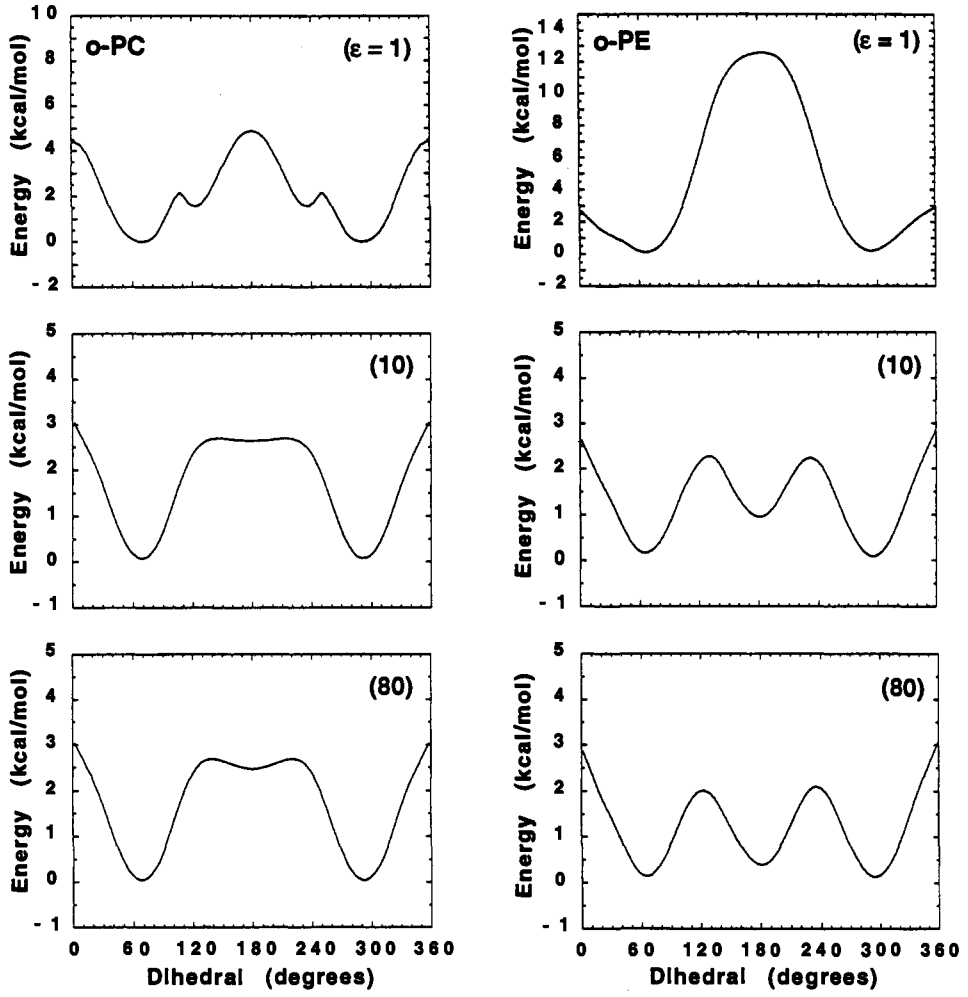

Figure 3. Potential of mean force, $W_{vac}(\alpha_5; \epsilon)$, calculated with dielectric constants ϵ of 1, 10, and 80.

Table 3. Stable Conformers in Vacuum

system	dielectric constant ϵ	conformation	energy (kcal/mol)	α_4 (deg)	α_5 (deg)
o-PC	1	gauche-1	0.0	249	67
	1	gauche-2	0.9	53	74
	1	gauche-3	2.8	291	124
	10	gauche	0.0	227	66
	10	trans	6.5	274	175
	80	gauche	0.0	223	67
	80	trans	6.3	180	180
o-PE	1	gauche-1	0.0	276	67
	1	gauche-2	1.5	50	41
	10	gauche	0.0	244	66
	10	trans	2.3	180	180
	80	gauche	0.0	185	64
	80	trans	0.5	180	180

1, shown in Figure 2, are similar to the *ab initio* surfaces calculated by Pullman et al.[41,42]

The progressive influence of the shielding of the intramolecular electrostatic interactions on the accessible dihedral conformations can be observed by comparing the adiabatic surfaces with ϵ values of 1, 10, and 80. It is observed from the adiabatic surfaces of Figure 2 that the α_5 trans barrier is decreased and the α_4 dependence becomes much flatter with ϵ = 10 or 80. The existence of broad gauche conformers and an increased stability for the trans conformer becomes apparent. The *o*-PE trans state is however considerably more stable than that of *o*-PC. In accord with the adiabatic surfaces, the PMF surfaces, shown in Figure 3, have local minima for α_5 in the gauche and trans conformation, although the trans conformation is again more stable in the case of *o*-PE. The shielding of electrostatic interactions with ϵ = 80 produces the stabilization of the trans conformation, yielding a trans/gauche energy difference of +2.4 and +0.3 kcal/mol for *o*-PC and *o*-PE, respectively. The secondary minimum observed in $W_{vac}(\alpha_5; \epsilon = 1)$ of *o*-PC is no longer present in $W_{vac}(\alpha_5; \epsilon = 80)$.

o-PC and o-PE in Bulk Water. In this section, the main results concerning the flexibility of *o*-PC and *o*-PE in bulk water, i.e., the solvation structure, the PMF $W_{bulk}(\alpha_5)$, and the isomerization rate constants, are described. The solvent radial distribution functions, $g(r)$, calculated from the trajectory in the 18-Å-radius water sphere, for the four oxygens surrounding the phosphate group, for the phosphate itself, and for the nitrogen, are shown in Figures 4 and 5. It is observed that the water structure around the phosphate group is very similar in *o*-PC and *o*-PE, although the radial distribution around the O12 oxygen, which is along the bonded direction from P toward N, is different. For both *o*-PC and *o*-PE, the O13 and O14 oxygens have very sharply peaked distribution functions, with an integrated population of three waters being found inside the first shell (within 3.2 Å). The O11 and O12 oxygens do not have such well-defined hydration shells. In contrast, the water structure around the N group is very different from the *o*-PC to the *o*-PE, with *o*-PE having a smaller number of waters that are packed more tightly. Figure 6 shows in stereo images the typical water structure around both molecules. In particular, the three waters tightly associated with the O13 and O14 oxygens can be seen clearly. Similar observations were made about the radial distribution around the headgroups of a DLPE bilayer (see Figure 7 of ref 12 and Figure 5 of ref 13).

The PMF $W_{bulk}(\alpha_5)$, calculated with umbrella sampling in a water sphere of 13-Å radius, is shown in Figure 7. The main

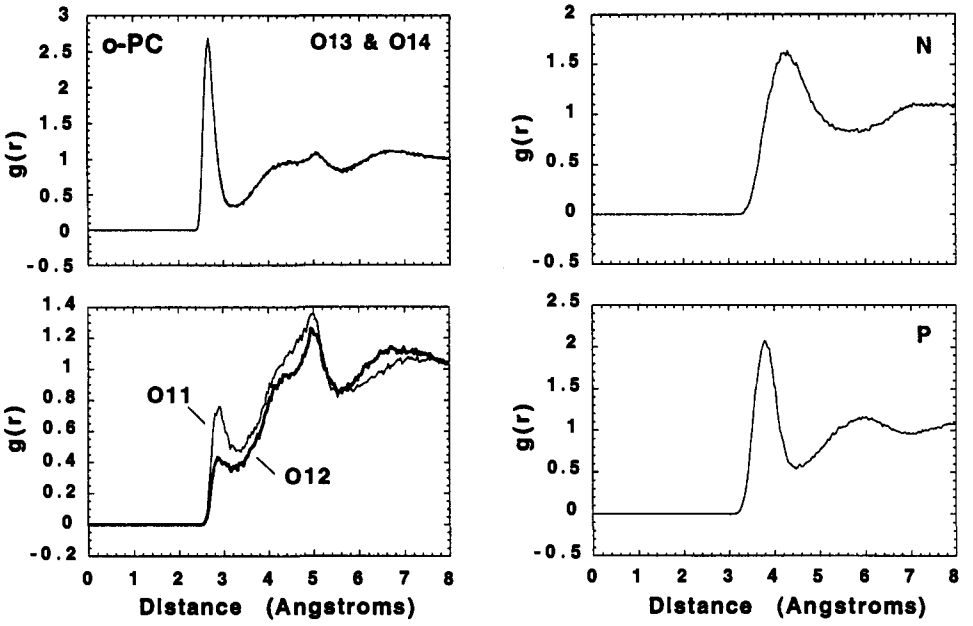

Figure 4. Radial distribution functions of the water structure around the *o*-PC molecule in bulk water. For both *o*-PC and *o*-PE, eight waters were found in the primary hydration shell of the phosphate group: three each about the free oxygens and one each about the bound oxygens; *o*-PC had 12 waters in the primary shell at 4.8 Å around the N, while the *o*-PE group had five waters at 3.6 Å (see also Figure 5).

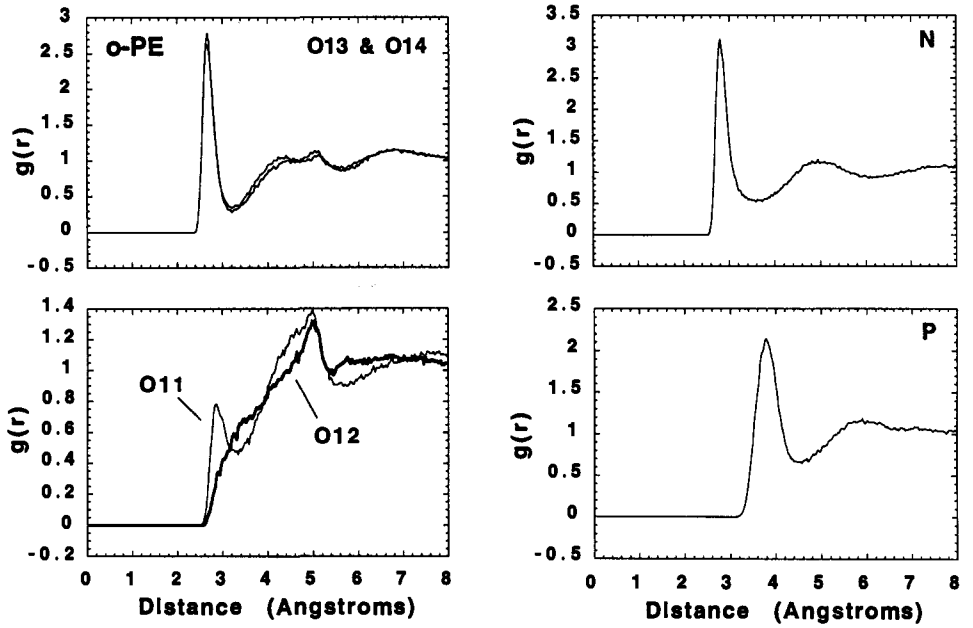

Figure 5. Radial distribution functions of the water structure around the *o*-PE molecules in bulk water (see also Figure 4).

features of the PMF are given in Table 2. It is observed that the influence of solvent results in a stabilization of the trans conformation relative to vacuum (see $W(\alpha_5; \epsilon = 1)$ in Figure 3). From $W_{bulk}(\alpha_5)$, trans/gauche energy differences of +1.5 and +0.02 kcal/mol are found for *o*-PC and *o*-PE, respectively. Although the trans and the gauche conformations are stable for both *o*-PC and *o*-PE in bulk water, there is a very shallow minimum in the PMF of *o*-PC in the trans conformation. The barrier in the cis conformation is higher for *o*-PC due to the much larger size of the N group.

The transition rate constants and the dihedral diffusion constants, calculated at the transition states using eqs 3, 5, and 6 from the velocity autocorrelation function obtained from trajectories of *o*-PC and *o*-PE, are summarized in Table 4.

***o*-PC and *o*-PE with Primary Hydration Waters.** The calculated PMF, $W_{prim}(\alpha_5; n = 11)$ and $W_{prim}(\alpha_5; n = 20)$, are shown in Figure 8 for *o*-PC and *o*-PE. The main features of the PMF with 20 primary waters are given in Table 2. For *o*-PC, the PMF values calculated with 11 and 20 primary waters are qualitatively similar to the PMF calculated in bulk water, though the result with 20 waters is closer to that in the bulk. With 20 waters, a shallow well is observed in the trans state, with an energy of 1.8 kcal/mol above that of the gauche state. For *o*-PE, a larger variation is observed as a function of the number of primary waters. With only 11 waters, the trans state is almost 4 kcal/mol higher than the gauche state and is relatively unstable. Increasing the number of primary waters to 20 yields a PMF resembling that observed in bulk solution. The trans state is stable, and its energy is 1.5 kcal/mol above that of the gauche state. Thus, one result of this numerical experiment is that a certain minimum number of nearby waters is sufficient to provide an adequate shielding of the strong attractive interaction between the P and the N groups and generate conformations similar to those appearing in solution.

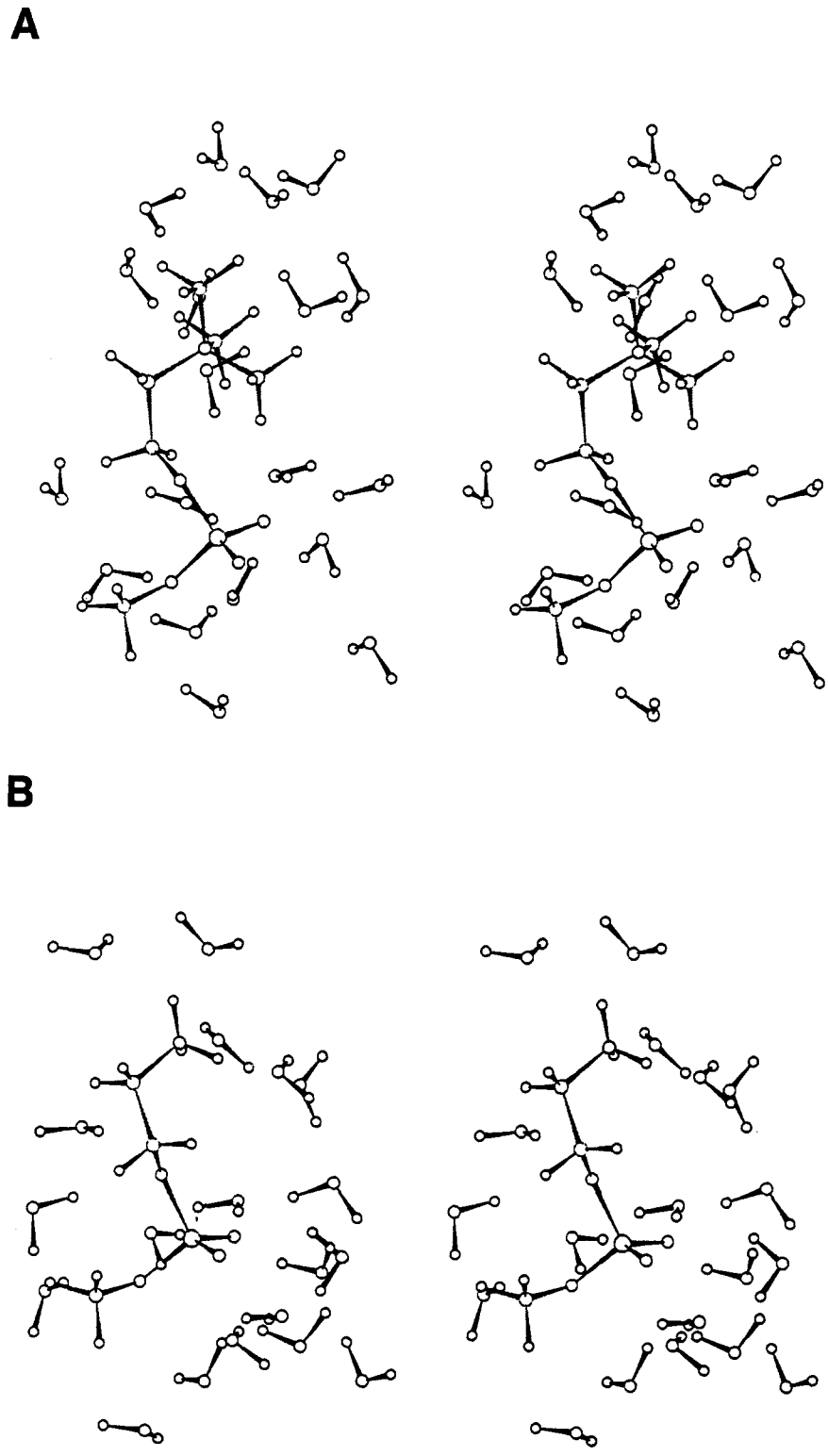

Figure 6. Stereo images showing the water structure in the primary hydration shell around *o*-PC and *o*-PE. Three waters strongly hydrogen bonded to O13 and O14 of the phosphate group and can observed in both figures. The dihedral angles for the *o*–PC group are $\alpha_2 = 297$, $\alpha_2 = \alpha_3 = 300$, $\alpha_4 - 210$, and $\alpha_5 = 81$; for the *o*–PE group the dihedral angles are $\alpha_2 = 288$, $\alpha_3 - 109$, $\alpha_4 = 170$, and $\alpha_5 = 288$.

Analysis and Discussion

As can be observed from Figures 2 and 3, the *o*-PC and *o*-PE molecules in vacuum with a dielectric constant of 1 are restricted to a few conformations separated by large energy barriers. The adiabatic potential energy surface shows a trans conformation dominated by a large electrostatic barrier. Similarly, the potential of mean force calculations show that the trans state has become an unstable barrier. In bulk water, the picture is completely different. The influence of solvent results in a stabilization of the trans conformation, yielding a trans/gauche energy difference of +1.5 and +0.02 kcal/mol for *o*-PC and *o*-PE, respectively. Thus, the conformational equilibrium resulting from the calculated PMF in bulk water indicates a population of molecules in the trans conformation that is only 4% for *o*-PC, while it is 31% for *o*-PE. This result is in qualitative agreement with experimental estimates for the relative populations obtained from solution NMR. Akutsu and Kyogoku used an analysis of spin–spin *J*-coupling constants to estimate an α_5 gauche/trans energy difference of 1.3 kcal/mol

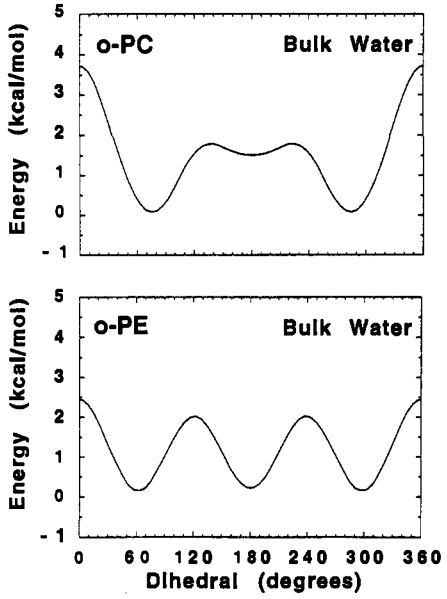

Figure 7. Potential of mean force $W_{bulk}(\alpha_5)$ calculated with 253 (*o*-PC) and 254 (*o*-PE) explicit TIP3 waters, using the umbrella sampling technique. The sampling was performed in 10-deg increments, and the final curve was symmetrized about 180° to increase the statistical convergence (see computational details). The PMF is plotted with Kaleidagraph using a weighted smoothing function.

Table 4. Transition Rate Constants in Bulk Solution

	o-PC	*o*-PE
Properties		
diffusion constant (deg²/ps)		
D_{eff} g, t barrier	1075	1700
D_{eff} g,g cis-barrier	2100	2250
Transition Rate[a] (ns^{-1})		
t → g	152 (1211)	33 (112)
g → t	22 (176)	36 (122)
$g_+ \rightarrow g_-$	2.5 (9.6)	20 (56)

[a] TST rates, calculated with eq 6, are given in parentheses.

for the *o*-phosphorylethanolamine molecule.[43] Although *o*-phosphorylcholine was also investigated by these authors, an estimate of its gauche/trans energy difference was not obtained. Hauser et al. estimated an α_5 gauche/trans energy difference of at least 2.7 kcal/mol for the PC headgroup in solution from an NMR study of DPPC, LPPC, and DHPC.[11] Their analysis indicated that the conformation of the PC headgroup is independent of the solvent used and of the state of aggregation (above and below the cmc), suggesting that it is mainly determined by intramolecular forces.[11] The α_5 dihedral angle is found exclusively in the gauche state in the known crystal structures of both PC and PE phospholipids.[5,44] The results of Akutsu and Kyogoku[43] and the present calculations suggest that, for the PE headgroup, this may be an effect of the low hydration state of the crystals, since the lack of solvent shielding changes the trans state from a minimum to an unstable barrier. The origin of the trans barrier is mainly electrostatic and results from a loss of the intramolecular interaction between the P and the N group. The trans conformation, in which the P-to-N distance is the largest, is highly unfavorable in vacuum, with a dielectric constant of 1. Reducing the electrostatic interactions artificially by setting the value of ϵ to 10 or 80 progressively reduces the barrier and increases the stability of the trans conformation. In the later case, the trans/gauche energy differences are 2.4 and 0.3 kcal/mol for *o*-PC and *o*-PE, respectively, which are similar to the values obtained in bulk water. Comparison of $W_{vac}(\alpha_5;\ \epsilon = 1)$ with $W_{bulk}(\alpha_5)$ demonstrates that solvation can effectively lower the electrostatically dominated trans barrier.

An interesting structural point is the observation that the α_5 gauche state for *o*-PC and *o*-PE is not at the same angle. This can be seen by considering the time series and the PMF in bulk water, shown in Figures 7 and 9. For *o*-PE, the average value of α_5 in the gauche state is around 63°. In contrast, the average α_5 is larger and around 77° for *o*-PC. A similar difference was also suggested by Akutsu and Kyogoku, based on an interpretation of the *J*-coupling constants for *o*-PC, *o*-PE, GPC, GPE, and both DPPC and DPPE bilayers.[43] The difference in the dihedral values appears to be due to the hydration structure around the P and N groups rather than simply the difference in size of the N group in *o*-PC and *o*-PE. This can be seen by observing that the location of the minimum seen in the adiabatic maps and in $W_{vac}(\alpha_5;\ \epsilon)$, shown in Figures 2 and 3), is nearly the same for both *o*-PC and *o*-PE, while it differs more markedly when the molecules are sufficiently hydrated, i.e., in the α_5 time series, in $W_{bulk}(\alpha_5)$, and in $W_{prim}(\alpha_5)$ with 20 primary waters (see Figures 7–9).

The solvation-induced increased flexibility is also reflected in the dynamics of *o*-PC/*o*-PE in bulk water. To better characterize the time scales involved in the conformational fluctuations, transition rate constants of *o*-PC and *o*-PE in bulk water were estimated using a high friction limit approximation based on eq 3. The results are given in Table 4. The dihedral diffusion constants about the α_5 angle, calculated using eq 5 at the gauche–trans and at the cis barriers, are 1075 and 2100 deg²/ps for *o*-PC and 1700 and 2250 deg²/ps for *o*-PE. The calculations show that the transition rates are overestimated by a factor of 3–8 by TST, indicating that the nature of the motions at the barrier top is diffusive. The transition rates are less overestimated by TST at the cis barrier because its curvature, W_b'', is larger and frictional effects, $1/D_b$, are less pronounced (see eq 3). The magnitude of the diffusion constants determined for the two barriers along α_5 for *o*-PC and *o*-PE can be understood qualitatively in terms of a simple argument. Considering the dihedral angle of four bonded atoms in the trans state, a slight displacement δd of the first and fourth atoms by a diffusive process results in a change in dihedral angle $\delta\phi$ of $\delta\phi^2 \simeq 2\delta d^2/L$, where $L = b\sin(\theta)$ is the perpendicular distance between two atoms separated by a bond length of b, θ is the bond angle, and D is the atomic diffusion constant. Neglecting hydrodynamic interactions in a free draining approximation, an effective dihedral diffusion constant can be defined as $2D/b^2\sin^2(\theta)$ (the factor of 2 arises from the relative diffusion of two particles). Assuming a value of 0.5 Å²/ps for D and 1.5 Å and 120° for θ, a dihedral diffusion constant on the order of 2000 deg²/ps is obtained, similar to the values obtained from the correlation function analysis. The dihedral diffusion is faster in *o*-PE than in *o*-PC since the N group diffuses more rapidly (smaller hydrodynamic radius). The larger diffusion constant at the cis barrier relative to the gauche–trans barrier can be partly understood as a consequence of the change in solvent-exposed surface area of the N group between these two conformations. Because of its larger size, the change in solvent-exposed area of the N group is larger for *o*-PC than for *o*-PE, reflecting the relative change in calculated diffusion constants. This is in accord with a study of pair diffusion in a simple Lennard–Jones fluid showing that the frictional solvation forces are dominated by the short-range structure and are proportional to the solvent-exposed surface.[45] However, the magnitude of the change in solvent-exposed area is on the order of 10%, while the diffusion constant of *o*-PC varies by a factor of 2, indicating that other factors are important. Nevertheless, since the magnitude of the diffusion constant has a relatively small dependence on the conformational state of the molecules, the relative time scale of the isomerization rate is mostly determined by the free energy

(43) Akutsu, H.; Kyogoku, Y. *Chem. Phys. Lipids* **1977**, *18*, 285–303.
(44) Hauser, H.; Pascher, I.; Pearson, R. H.; Sundell, S. *Biochem. Biophys. Acta* **1981**, *650*, 21–51.
(45) Straub, J.; Berne, B.; Roux, B. *J. Chem. Phys.* **1990**, *93*, 6804–6812.

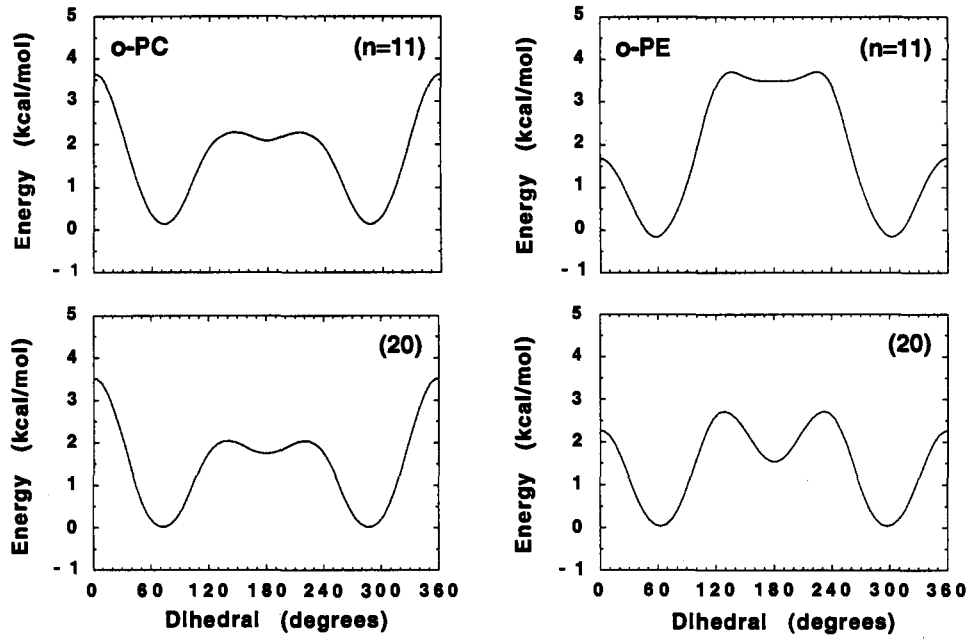

Figure 8. Potential of mean force $W_{prim}(\alpha_5; n)$ calculated with 11 and 20 primary waters about *o*-PC and *o*-PE to determine the relative effect of the close waters on the free energy surface.

barriers of the PMF. The largest change due to the variation of the diffusion constant represents only a factor of 2 in the case of *o*-PC.

The nature of the conformational fluctuations of *o*-PC and *o*-PE in water is illustrated by the time evolution of the dihedral angles during the unrestrained trajectory performed in the 18-Å-radius water sphere. Figure 9 shows the time series of α_4 and α_5 during the trajectories. In both cases, there is considerable exploration of much of the α_4 dihedral conformation space. In contrast, the α_5 of both molecules spends the majority of its time confined to a few major conformations. In the case of the *o*-PE molecule, in addition to the two gauche states, there is also time spent in the trans state. For *o*-PE, a gauche to trans and a trans to gauche transition in and out of the trans state occurs at 51 and 147 ps, and a transition through the cis state into the other gauche state occurs at about 392 ps. The α_5 of *o*-PC spends almost the entire simulation in a single gauche state. Near 500 ps, a series of transitions from gauche to the opposite gauche, back to gauche, and then again back to the opposite gauche occur. Although such rare events are not statistically significant, they provide useful information: A detailed examination of the water–headgroup interactions in the transition of the *o*-PC molecule determined that the transition from gauche to trans was initiated through fluctuations in the number of waters hydrogen bonded to the O13 and O14 oxygens. For most of the simulation, these two oxygens had three water molecules associated with them. Just before the transition, O13 lost two of these hydrogen bonds to water, both of which were subsequently regained with different waters in the trans state. Meanwhile, O14 also lost a single hydrogen bond and regained that bond in the trans state with a different water. The mean residency time for a hydrogen bond from water to O13 or O14 was 50 ps, but there was considerable variability, with one or two of the waters being very tightly associated and the third being less tightly associated. Although such a comparison is not rigorous, it can be noted that the α_5 time series shown in Figure 9 are qualitatively in accord with the calculated PMF and transition rate constants. During the trajectory, *o*-PC and *o*-PE spent 5 and 16% in the trans state, to be compared with the 4 and 31% population ratio extracted from $W_{bulk}(\alpha_5)$; the average time spent in the trans conformer is much shorter for *o*-PC than for *o*-PE.

The influence of the solvent on the conformational equilibrium may be interpreted according to two somewhat opposite views. The influence of solvent results in a "continuum-like" shielding of the intramolecular electrostatic interactions; the PMF $W_{vac}(\alpha_5; \epsilon = 80)$, calculated in vacuum with electrostatic interactions shielded by setting the dielectric constant to 80, and the PMF $W_{bulk}(\alpha_5)$, calculated in bulk water, exhibit a qualitatively similar gauche/trans energy difference. On the other hand, the radial distribution function (see Figures 4 and 5) and the dynamics of the hydration waters during the dihedral transitions (see above) reveal important structural features in the hydration around the P and N groups. In particular, a small number of waters are strongly associated with the phosphate group. To gain further insight into the relative role of "continuum-like" dielectric shielding versus nearest "hydration waters" on the internal flexibility of the *o*-PC/*o*-PE molecules, numerical experiments were performed using model systems with reduced primary hydration. The calculated PMF values with reduced systems, $W_{prim}(\alpha_5; n = 11)$ and $W_{prim}(\alpha_5; n = 20)$, clearly indicate that including 20 water molecules around the polar groups of *o*-PC and *o*-PE is sufficient to decrease the large intramolecular electrostatic barrier. A similar approach to account for the dominant effects of bulk solvation by including a small number of waters around the most polar groups has been used in *ab initio* calculations.[41,42] Pullman et al. studied the flexibility of *o*-phosphorycholine and *o*-phosphorylethanolamine in the presence of five or six waters around the phosphate group.[41,42] As expected, their calculations did not exhibit the stabilization of the trans conformer observed in bulk solution. Although five or six waters strongly bound to the phosphate group are observed during the trajectory in bulk solution (see Figures 4 and 5), the present calculations with the reduced model systems demonstrate that this number is not sufficient. To reproduce the qualitative features of "bulk-like" solvation, it is necessary to provide also the primary hydration for the N group. The present calculations with reduced model systems indicate that below approximately 20 waters/headgroup the intramolecular electrostatic interactions are not sufficiently shielded and the intrinsic flexibility of the polar heads is reduced.

It is interesting to note that the number of primary hydration water molecules necessary to reproduce the qualitative features of "bulk-like" solvation intramolecular flexibility seems to parallel some recent NMR experimental results in bilayers. Several studies were concerned with the effect of hydration level on the measured NMR properties of PC/PE systems. Ulrich et al. showed that the $T1$ relaxation times of multibilayer dispersions

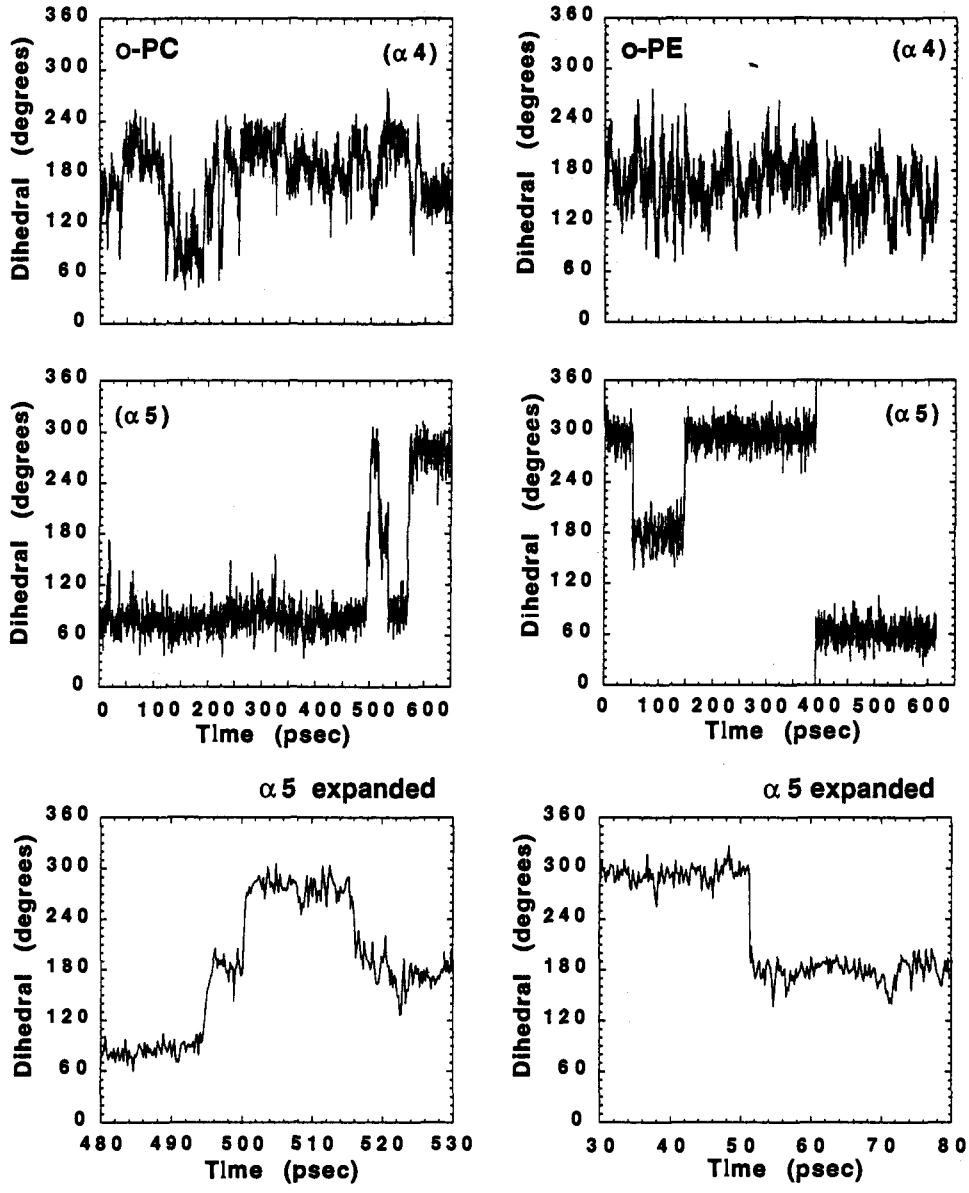

Figure 9. Time series of α_5 and α_4 for both o-PC and o-PE molecules from the molecular dynamics trajectory in bulk water. The o-PC molecule spent 81% of the simulation time in the gauche state near 67°, 14% of the simulation time in the opposing gauche state, and 5% of the time in the trans state. The o-PE molecule spent 36% of the simulation time in the gauche state near 60°, 48% of the time in the opposite gauche state, and 16% of the time in the trans state. The bottom part of the figure shows transitions of the o-PC and o-PE groups on an expanded time scale.

of DOPC were much reduced below 20 waters per headgroup.[10] Bechinger and Seelig, working with bilayers of POPC deuterated at the methylene segments, showed a counterdirectional change of the quadrupole splitting as the water was decreased below 20 waters per headgroup. Although the experimental measurements were obtained from bilayer systems in which lipid–lipid interactions were important while the present study considered isolated molecules in solution, they both suggest that a minimum number of water molecules is necessary to solvate the headgroups. The primary waters are very strongly bound to o-PC and o-PE and provide a large fraction of the solvation energy. On the basis of the microscopic model, 20 primary waters can provide 70 and 80% of the total solvation energy in bulk water of o-PC and o-PE, respectiveiy. The larger contribution for o-PE is due to the smaller size of the N group, giving rise to a stronger association with the nearest water molecules. Because the primary water molecules are so strongly associated with o-PC and o-PE, it is interesting to consider the properties of the hydrated headgroup as a single supramolecule. The surface areas, volumes, and dipoles of the model systems with and without the 20 primary waters are given in Table 5. In particular, the dipole in the presence of primary waters is significantly reduced for o-PE in contrast to the o-PC. This is a consequence of the strong hydrogen bonding of the waters with the ammonium group, in contrast to the weaker association with the choline group of o-PC. This suggests that in bilayers the effective dipole of the PE polar head may be significantly shielded by the primary hydration shell. Finally, the gauche to trans relative differences in volume and surface area of the reduced systems do not parallel that of the vacuum systems.

Table 5. General Properties of o-PC and o-PE

	PC		PE	
property[a]	gauche	trans	gauche	trans
effective volume (Å^3)	497	485	417	409
	1292	1326	1286	1218
effective area (Å^2)	346	371	307	312
	699	717	703	663
dipole (eÅ)	5.2	5.6	3.9	5.9
	4.2	3.7	1.1	1.2

[a] First line gives the molecules in vacuum; second line gives averages including the 20 primary waters.

It's intriguing to speculate that the extra flexibility of the PE head groups relative to the PC headgroups, reached with a small number of hydration waters, may be reflected in the physical state and the thermodynamic behavior of bilayers. Two conformers, gauche-plus and gauche-minus, are energetically accessible for hydrated PC, while the trans conformer is also significantly populated for hydrated PE. Bulk-like conformational equilibrium is qualitatively reproduced in the presence of approximately 20 primary waters. The packing and excluded volumes resulting from the various hydrated conformers are different (see Table 5). The importance of the primary hydration waters suggests that elementary properties of the hydrated molecules such as the excluded volume, area, and dipoles are more meaningful than the properties of the bare molecules in vacuum.

Conclusion

In this paper, the importance of solvation on the conformational flexibility of *o*-phosphorylcholine and *o*-phosphorylethanolamine, model compounds for the two most common phospholipid headgroups, was investigated with a fully detailed atomic model. The calculations reveal the important role of solvent in reducing strong intramolecular electrostatic energies. In vacuum, the trans conformation, in which the P-to-N distance is the largest, is unstable and strongly disfavored with respect to the gauche conformations due to loss of intramolecular electrostatic interactions. In bulk water, the influence of solvent results in a stabilization of the trans conformation, yielding a trans/gauche energy difference of +1.5 and +0.02 kcal/mol for *o*-PC and *o*-PE, respectively. The calculations indicate that, in bulk water, the population of *o*-PC molecules in the trans conformation is significantly smaller than that of *o*-PE, i.e., 4 and 31% for *o*-PC and *o*-PE, respectively, a result that is in qualitative agreement with experimental NMR estimates from an analysis based on *J*-coupling constants by Akutsu and Kyogoku[43] and Hauser.[11] More generally, it may be expected that the conformational flexibility of similar polar molecules, with strong intramolecular electrostatic interactions, would be affected similarly by hydration.

Further insight into the nature of hydration effects was gained by considering simplified model systems in which the influence of solvent was approximated by a vacuum continuum dielectric constant and by including a small number of explicit primary hydration water molecules solvating the P and N groups. It is observed, from the calculated PMF of *o*-PC and *o*-PE with the approximate solvent models, that a vacuum continuum dielectric constant of 80, or the presence of 20 explicit water molecules around the polar group, is sufficient to stabilize the trans conformation and reproduce qualitatively the behavior found in bulk water. This suggests that the solvent-induced increased intramolecular conformational flexibility may be equivalently interpreted in terms of "continuum-like" dielectric shielding or structuration effects by the primary hydration shell. On a methodological note, similar comparisons with other approximate treatment of solvation not considered here, such as a distance-dependent dielectric constant,[28] could also be attempted.

The present approach could be extended to investigate the influence of ions and charged molecules on the conformation of the common polar headgroups. There is much current interest in the effects of charged molecules on the headgroups in phospholipid bilayers.[46-51] Charged substances induces changes in the deuterium quadrupole splitting and the phosphate CSA, which have been interpreted as representing a change in the tilting angle of the P–N dipole. An important question, which remains unanswered, is whether the influence of ions and charged molecules on the headgroups results from the presence of the membrane–solution interface or whether it is due to specific ion–lipid interactions. In other words, are there intramolecular conformational changes induced by charged substances on model compounds such as *o*-PC and *o*-PE? Akutsu and Nagamori suggest from DPPC bilayer quadrupole splitting and infrared Raman studies that cations induce a change from about 80° to about 65° for α_5.[51] This is in contrast to the suggestions from other groups, that the effect of the charge is to induce a change in the P–N dipole and no intrinsic conformational shift.[46-50] Molecular dynamics simulations and NMR *J*-coupling experiments on *o*-PC and *o*-PE molecules in bulk solution could provide detailed information on the influence of charged molecules on these compounds. Further theoretical and experimental investigations are planned toward understanding the effects of charged substances on *o*-PC and *o*-PE.

Acknowledgment. We are grateful to A. D. MacKerell, Jr., and M. Karplus for providing the PARM 22 lipid parameter set prior to publication. T.B.W. is supported by a GRTM fellowship. B.R. is a FRSQ fellow.

Supplementary Material Available: CHARMM topology and parameter files used in the present calculations (4 pages). This material is contained in many libraries on microfiche, immediately follows this article in the microfilm version of the journal, and can be ordered from the ACS; see any current masthead page for ordering information.

(46) Seelig, J.; Macdonald, P. M.; Scherer, P. G. *Biochem.* **1987**, *26*, 7535–7541.
(47) Scherer, P. G.; Seelig, J. *EMBO* **1987**, *6*, 2915–2922.
(48) Marassi, F. M.; Macdonald, P. M. *Biochemistry* **1991**, *30*, 10558–10566.
(49) Roux, M.; Neumann, J. M.; Hodges, R. S.; Devaux, P. F.; Bloom, M. *Biochem.* **1989**, *28*, 2313–2321.
(50) Roux, M.; Bloom, M. *Biochemistry* **1990**, *29*, 7077–7089.
(51) Akutsu, H.; Nagamori, T. *Biochemistry* **1991**, *30*, 4510–4516.